Accepted at 23rd International Conference on Advanced Communications Technology, IEEE/ICACT 2021

Adaptive Millimeter-Wave Channel Estimation and Tracking

Mohammadreza Robaei*, Robert Akl*, Robin Chataut† and Utpal Kumar Dey*
*Department of Computer Science and Engineering, University of North Texas, Denton, TX, USA
†Computer Science Department, Fitchburg State University, Fitchburg, MA, USA
*mohammadreza.robaei@unt.edu, *robert.akl@unt.edu, †rchataut@fitchburgstate.edu, *utpal-kumar.dey@unt.edu

***Abstract*—Computationally efficient channel estimation is critical to optimize the capacity of millimeter-wave communication network. For this, compressed-sensing has been recommended to estimate a few dominant channel parameters. However, it is challenging to extend compressed-sensing solutions to a continuous channel tracking due to the number of required measurements. In this paper, we propose efficient adaptive channel estimation and tracking for millimeter-wave communication with minimum communication overhead. We recommend characterizing the instantaneous rate of change of the millimeter-wave channel as a gradient of spectral overlap between channels. The significant channel variations are then detected locally by applying convergence in mean square sense to the resultant time sequence. If the channel experiences significant variation, then the multipath components are estimated directly using compressed-sensing. Otherwise, the channel parameters are updated using the channel tracking model. For this purpose, we introduce an efficient channel tracking model based on small-angle assumption. The proposed channel tracking method employs an autoregressive process to update the angle of departure and angle of arrival. We present numerical results to evaluate the proposed adaptive channel estimation and tracking method.**

***Index Terms*—Millimeter-wave massive MIMO, channel tracking, channel estimation, channel variation rate, convergence in mean square**

I. Introduction

Millimeter-wave and massive MIMO are the two technologies that can fulfill specifications of the IMT-2020 vision. Millimeter-wave communication can provide large bandwidth thanks to the high carrier frequency. For example, centered around 28GHz, the n257 operation band can provide 3GHz bandwidth [1]. On the other hand, massive MIMO has been proposed to increase the spectral efficiency of the network. Besides, massive MIMO is necessary to overcome the propagation challenges of the millimeter-wave communication by enabling directional communication. Nevertheless, beamforming leads to a sparse channel with a few dominant components.

Minimum Mean Square Error (MMSE) method is widely applied to estimate MIMO channels in the sub-6GHz band [2]. The number of required pilots signals to estimate millimeter-wave channel using MMSE is in the order of $\mathcal{O}(NrNt)$, where N_t and N_r are the transmitter and receiver antenna sizes. Since the N_t and N_r can be very large, MMSE is not an efficient way to estimate the large sparse channel. For sparse channel, it would be much more efficient computationally if we can estimate only the dominant components. For this purpose, compressed-sensing techniques have been recommended for millimeter-wave MIMO channel estimation [3], [4]. It has been shown that the Orthogonal Matching Pursuit (OMP) algorithm only needs $\mathcal{O}(s \ln(N_r N_t))$ measurements to estimate a signal with an s non-zero components.

The compressed-sensing-based channel estimation methods are applied to the block fading channel models [3][5]. In this model, it is assumed that the channel experiences the same fading for some interval of time. In a block fading channel model, each channel realization is a random process taking place independent of the previous channel realizations. Hence, each channel realization needs to be estimated independently. Due to the required number of measurements, continuous channel estimation introduces substantial pilot overhead restricting the channel Spectral Efficiency (SE).

If the channel varies smoothly, it is possible to leverage the channel's prior knowledge to update the dominant components instead of estimation. We call this scheme channel tracking. The ultimate goal is to update the Angle of Departure (AoD) and Angle of Arrival (AoA) using a minimum number of measurements. In [6], authors have recommended a channel tracking algorithm using the Kalman filter. Although the estimation performance is promising, the recommended algorithm shows severe degradation as the angular noise increases. Rodriguez et al. [7] have addressed channel tracking using the maximum-likelihood estimator, where each pair of AoD and AoA is calculated using a gradient of previously estimated estimated AoD and AoA pairs.

In [8], the linear model has been recommended considering the linear angular variation under spatial consistency. A similar approach has been adopted by NYUSIM [9] to simulate continuous millimeter-wave channel. The variant angle model can be used to update multipath components if the geometry of the road dictates the local direction of the user.

In [10], millimeter-wave channel tracking using side-channel information has been recommended for vehicular communication. The recommended method solves the state-space problem to calculate the speed and position of User Terminal (UT). The initial state is obtained using on-board sensors, such as GPS.

In this paper, we utilize spatial consistency to generate continuous linear time-variant channel realizations. Under spatial consistency, the channel realizations that are sampled temporally close are correlated. It has been shown that the Correla-

tion Matrix Distance (CMD) can measure this correlation by finding the spectral overlap between the channel realizations [11]. In [12], authors have examined CMD as a metric to measure the channel variation under spatial consistency. We have four contributions as in the following:

- The channel variation is defined as a spectral overlap between the channels, and it is measured using CMD. Then, we propose to measure the instantaneous rate of change of the channel as the gradient of the CMD sequence.
- We employ Convergence in Means Square to detect local significant channel variation. If the channel shows significant variation, the multipath components are estimated using the OMP algorithm. Otherwise, the multipath components are updated through channel tracking.
- We model AoD and AoA as autoregressive processes to update antenna steering vectors for channel tracking
- Computationally efficient channel tracking model using small-angle assumption has been introduced to update multipath components

The following notation is used in the paper. a is scalar, and $\overline{a}$ is vector. A stands for matrix, and I is an identity matrix. $\otimes$ is Kronecker product, and $\circ$ represents Hadamard product. $\|A\|_F$ is the Frobenius norm of the matrix A. $(\cdot)^T$, $(.)^*$, $(.)^H$ are transpose, conjugate, and conjugate transpose. All vectors are column-wise. We use channel variation rate for instantaneous rate of change of the channel in the remaining of the paper. Table I summarizes important abbreviations.

II. Sparse Problem Formulation

The channel transfer function $H(t,f) \in \mathbb{C}^{N_r \times N_t}$ can be obtained as defined in (1) per cluster $p \; \forall\{0,1,\cdots,P-1\}$, per subpath $l \; \forall\{0,1,\cdots,L-1\}$, complex channel gain α, Doppler shift υ, and excess delay τ. All parameters are generated at random per cluster and per subpath. The transmitter and receiver steering vectors, $\overline{a}_t(\theta)$ and $\overline{a}_r(\varphi)$, are generated assuming ULA antennas with the separations of d_t and d_r as in (2) and (3), where θ and φ are the AoD and AoA.

$$H(t,f) = \sqrt{N_t N_r} \sum_{p=0}^{P-1} \sum_{l=0}^{L-1} \alpha_{p,l} e^{j2\pi \upsilon_{p,l} t} e^{-j2\pi f \tau_{p,l}} \times \overline{a}_r(\varphi_{p,l}) \overline{a}_t^H(\theta_{p,l}) \quad (1)$$

$$\overline{a}_t(\theta) = \left[1, e^{-j2\pi \frac{d_t}{\lambda} \sin(\theta)}, \cdots, e^{-j2\pi \frac{(N_t-1)d_t}{\lambda} \sin(\theta)}\right]^T \quad (2)$$

$$\overline{a}_r(\varphi) = \left[1, e^{-j2\pi \frac{d_r}{\lambda} \sin(\varphi)}, \cdots, e^{-j2\pi \frac{(N_r-1)d_r}{\lambda} \sin(\varphi)}\right]^T \quad (3)$$

The transfer function $H(t,f)$ can be mapped into its sparse representation in angular domain using virtual channel model [13] and Discrete Fourier Transform matrices A_t and A_r as represented in (11). The columns of the A_t and A_r are the orthogonal basis that discretize the angular domain in the transmitter and receiver, respectively.

$$H(t,f) = A_r H(t,a) A_t^H \quad (4)$$

TABLE I
List of Abbreviations

$\overline{a}_t(\theta)$, $\overline{a}_r(\varphi)$	Transmitter and receiver steering vectors
AoA, AoD	Angle of Arrival and Angle of Departure
CMD	Channel Matrix Distance
CMSV	Value measured using Convergence in Mean Square
$\overline{h}_v(t,a)$	Vectorized virtual channel
$H(t,a)$	Virtual channel
$H(t,f)$	Channel transfer matrix
NMSE	Normalized Mean Square Error
N_t, N_r	Transmitter and receiver antenna size
N_{trf}, N_{rrf}	Number of RF chains at the transmitter and receiver
OMP	Orthogonal Matching Pursuit
SE	Spectral Efficiency
UT	User Terminal

Both the transmitter and receiver are equipped with hybrid digital-analog beamforming. At each frame m, transmitter sends pilot sequence $\overline{x}_m$. We can compute received signal at the frame $m \in \{1,2,\cdots,M\}$ as represented in (5),

$$\overline{y}_m(t,f) = {W_m}^H H(t,f) F_m \overline{x}_m + {W_m}^H \overline{\vartheta}_m \quad (5)$$

where $F_m \in \mathbb{C}^{N_t \times N_{trf}}$ and $W_m \in \mathbb{C}^{N_{rrf} \times N_r}$ are the beamforming matrices. N_{trf} and N_{rrf} are the number of RF chains at the transmitter and receiver, and $\overline{\vartheta}_m \in \mathbb{C}^{N_{rrf} \times 1}$ is the noise vector.

We can reshape channel matrix $H(t,a)$ to a column vector $\overline{h}_v(t,a) \in \mathbb{C}^{N_t N_r}$ using Kronecker vectorization. We also define $\Phi_m = \left({\overline{x}_m}^T {F_m}^T \otimes {W_m}^H\right) \in \mathbb{C}^{N_{rrf} \times N_t N_r}$ as a projection matrix, $\Psi = (A_t^* \otimes A_r) \in \mathbb{C}^{N_t N_r \times N_t N_r}$ as a dictionary matrix, and $\overline{e}_m = {W_m}^H \overline{\vartheta}_m$ as filtered noise. Then, we can rephrase (5) as

$$\begin{aligned} \overline{y}_m &= \left({\overline{x}_m}^T {F_m}^T \otimes {W_m}^H\right) \otimes (A_t^* \otimes A_r) \overline{h}_v(t,a) + \overline{e}_m \\ &= \Phi_m \Psi \overline{h}_v(t,a) + \overline{e}_m \end{aligned} \quad (6)$$

Assuming that all M pilot sequences in the same block will experience the same channel, received signal $\overline{\mathbf{y}}$ can be formulated by concatenating all the measured signals as in (7). In (7), $\mathbf{\Phi}$ is the concatenated projection matrix and $\overline{\mathbf{e}}$ is the concatenated filtered noise.

$$\overline{\mathbf{y}} = \mathbf{\Phi} \Psi h_v(t,a) + \overline{\mathbf{e}} \quad (7)$$

III. Methodology

This section describes the proposed spectral overlap measurement, adaptive channel estimation-tracking, and convergence in mean square. If a significant non-stationary variation has been detected in the channel, then channel parameters are estimated using the OMP algorithm. Otherwise, channel parameters are updated using the proposed small-angle channel tracking model.

A. Correlation Matrix Distance

We may consider that there is a good correlation between channel realizations for channel coherent time. However, it is challenging to determine channel coherent time in practice. Instead, it would be helpful if we can measure channel variation with a time. We propose to leverage the correlation,

i.e., spectral overlaps between the channel realization, to characterize the dynamics of the channel. It is possible to measure variation and instantaneous rate of variation by tracking the spectral similarities between two channel realizations.

CMD, represented with D in (8), measures the spectral overlap between two channel realizations and assigns a scalar between zero and one, where zero means channels are identical, and one means channels are at the maximum distance from each other. In (8), $R(t) = H(t,a)H(t,a)^H$ is the receiver correlation matrix. Since the function of a random variable is also a random variable, CMD is a random variable that maps the $H(t,a) \in \mathbb{C}^{N_r \times N_t}$ to an interval $[0,1] \in \mathbb{R}$. The behavior of CMD sequence with a time provides information about channel's spectral variation.

$$D = 1 - \frac{tr\{R(t)\,R(t+\Delta t)\}}{\|R(t)\|_f \|R(t+\Delta t)\|_f} \tag{8}$$

B. Channel Estimation

In this paper, OMP algorithm [14] has been employed to estimate channel parameters. OMP algorithm estimates the s non-zero elements in $\overline{h}_v(t,a)$, iteratively. At each iteration, the residual of the received signal is projected on a transfer matrix $\mathbf{\Phi\Psi}$ to estimate the support, ω, corresponding to the maximum projection power. The number of iterations can be determined either by the number of non-zero elements in $\overline{h}_v(t,a)$, or by expected residual error. The union of the estimated supports defines the support set $\Omega = \{\omega_1, \omega_2, \cdots, \omega_s\}$ corresponding to the location of non-zero elements in $\overline{h}_v$, where $|\Omega| = s$. Then, the channel gains can be obtained applying the least-square approximation to the set of columns selected from $\mathbf{\Phi\Psi}$ corresponding to $\omega \in \Omega$.

The bandwidth of the channel is set to 50MHz, and it is divided into 64 subcarriers. We leverage common support assumption between subcarriers to apply majority voting and decrease the estimation error in low SNR regimes. This is important because the estimation error in the channel estimation may cause accumulated error in the channel tracking stage.

Applying OMP directly to each channel realization leads to pilot overhead. Alternative solutions are essential to extend discrete channel estimation to continuous channel tracking.

C. Channel Tracking

We aim to develop a channel tracking model that can utilize the prior knowledge about the channel to update AoD, AoA. We modify the channel transfer function in (1) to obtain the evolved transfer function in (9)

$$\begin{aligned} H(t+\Delta t, f) = \sqrt{N_t N_r} \sum_{p=0}^{P-1} \sum_{l=0}^{L-1} \alpha_{p,l}(t+\Delta t) \\ \times \overline{a}_r(\varphi_{p,l} + \Delta\varphi_{p,l}) \overline{a}_t^H(\theta_{p,l} + \Delta\theta_{p,l}) \\ \times e^{j2\pi\upsilon_{p,l}t} e^{-j2\pi f \tau_{p,l}} \end{aligned} \tag{9}$$

In (9) $\Delta\theta_{p,l}$ and $\Delta\varphi_{p,l}$ are path-wise AoD and AoA variations in a time interval of Δt, and they reflect the changes in the subpaths due to the UT mobility or the dynamics of the environment. We propose the following proposition to update channel parameters by assuming $\Delta\theta_{p,l}$ and $\Delta\varphi_{p,l}$ are small.

Preposition Channel evolution considering the geometric variation of the AoD and AoA pairs can be obtained using

$$H(t+\Delta t, f) = H(t,f) \circ \overline{a}_{\Delta\varphi} \circ \overline{a}_{\Delta\theta}^H \tag{10}$$

proof: See appendix

Preposition 1 updates channel transfer matrix with respect to small-angle assumption. For the channel realization $n+1$ (n represents index of a sample), the $\overline{a}_{\Delta\varphi}$ and $\overline{a}_{\Delta\theta}$ are updated in the form of autoregressive process as

$$\overline{a}_{n+1} = \overline{a}_n - \frac{1}{K} \sum_{k=0}^{K-1} \overline{a}_{n-k} + \overline{e}_n \tag{11}$$

where $\overline{e}_n$ represents the measurement noise. Substituting (10) in (4) gives the updated virtual channel.

We aim to show that (10) can be used to update channel realizations if the channel sampling rate is large enough to capture spatial correlation between the channel realizations.

D. Characterizing Instantaneous Rate of Change of Channel

The method we propose to detect a non-stationary change in the channel is based on the rate of channel's local variation. One can expect that for the slow varying channel under spatial consistency the local spread of the D to be highly concentrated in the region of zero. We can then define the channel variation rate as a gradient of D as defined in (12). In (12), G_K is the gradient of the CMD sequence within a window of size K.

$$G_K = \nabla D \tag{12}$$

The signal G_K has a J-shaped distribution with a compact histogram concentrated around zero. One can characterize the channel variation rate examining the components in the tail of the distribution. For this purpose, we employ the convergence in mean square sense. Since convergence in mean square implies convergence in probability, it also implies convergence in distribution. However, unlike convergence in probability, convergence in mean square is sensitive to the components in the tail. The convergence in mean square sense is defined by $\lim_{n\to\infty} \mathbb{E}\left[|G_n - \mathbb{E}[|G_n|]|^2\right] = 0$ such that $\mathbb{E}\left[|G_n|^2\right] < \infty$. We define a weaker inequality in (13), which allows us to apply convergence in mean square to more realistic signals.

$$\lim_{n\to\infty} \mathbb{E}\left[|G_n - \mathbb{E}[|G_n|]|^2\right] < \epsilon \tag{13}$$

While (13) holds locally for stationary channel with marginal channel variation, the violation of the inequality in (13) implies significant channel variation. As a result, we define inequality in (14) with $\epsilon = (\gamma\sigma_{G_K})^2$ to detect channel variation rate.

$$\max |G_{n-k:n} - \mathbb{E}[|G_{n-2k:n}|]|^2 > (\gamma\sigma_{G_K})^2,\ \forall k < K \tag{14}$$

In (14), σ_{G_K} represents the spread of G_K within a window of K. The variable, $\gamma \geqslant 0$, is a threshold determines the saddle point to estimate or track the channel parameters. For $\gamma = 0$, the algorithm decays to oracle channel estimation.

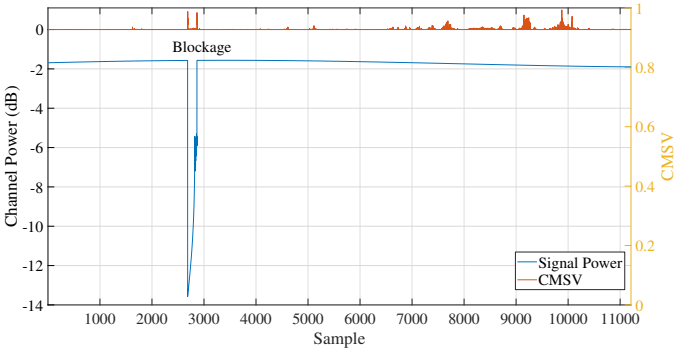

Fig. 1. Blockage event detection using convergence in mean square

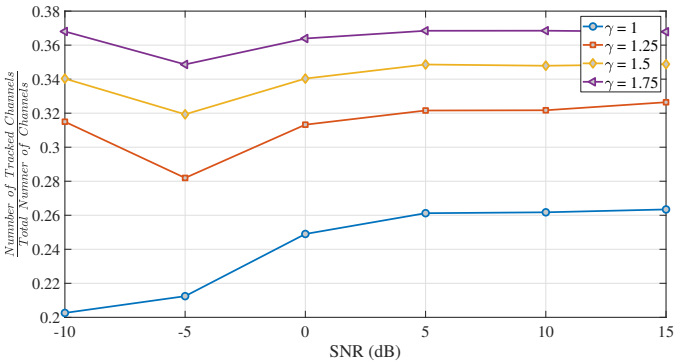

Fig. 3. The ratio of tracked channels to the total number of channels

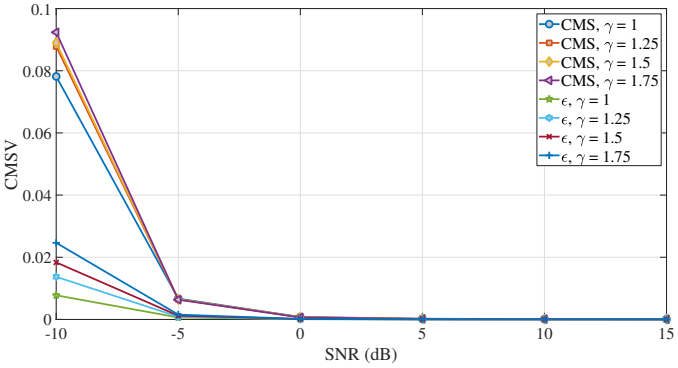

Fig. 2. CMSV and ϵ as a function of SNR

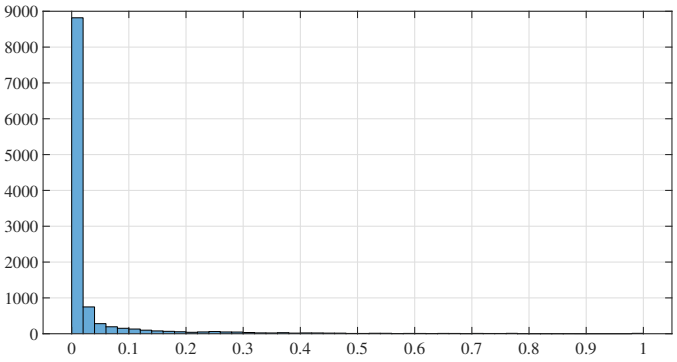

Fig. 4. Distribution of CMD

IV. Numerical Results

We assume that both the transmitter and the receiver are equipped with 16-element ULA antennas and 4 RF chains. The career frequency is 28GHz and the channel sampling rate is fixed to 1.2 samples per wavelength, equal to sampling interval of 9ms. In order to add significant non-stationary event, we added random blockage event recommended in [15] to a UT trajectory as shown in Fig. 1.

CMSV **-** Fig. 1 shows the blockage event detected by the convergence in mean square. It is shown the falling and rising edges of the blockage event are detected properly. In addition, channel variations due to other events such as antenna misalignment are detected along the UT trajectory.

We have observed that the CMSV is inversely proportional to the SNR. As shown in Fig. 2, at low SNR regimes without significant non-stationary event, we have measured larger CMSV, which indicates violation of stationarity. On other hand, for SNR$\geq$ 0, CMSV has been tightly concentrated around zero that points to a stationary behavior. We also have observed that CMSV can be as large as 0.9 at the blockage edges.

The ratio of the tracked channels to the total number of channels is shown in Fig. 3 for $M = 70$. This ratio is directly proportional to the SNR and gets saturated for SNR$\geq$ 0. The reason is that the G_K has a J-shaped distribution concentrated at zero with decaying tail, as in the Fig. 4. The decaying slope of the tail is directly proportional to the SNR, i.e., the distribution of G_K is more compact around zero at the higher SNR regimes. Consistent with this result, Fig. 2 shows that CMSV approaches zero as the SNR increases. At low SNR values, CMSV diverges from the ϵ indicating that as the SNR decreases the non-stationarity increases.

NMSE **-** The reconstruction error has been evaluated using Normalized Mean Square Error (NMSE) defined by $NMSE[dB] = 10\log_{10}\left(\frac{\|\overline{h}_v - \widehat{h}_v\|_2^2}{\|\overline{h}_v\|_2^2}\right)$ for vectorized channel $\overline{h}_v$ and estimated/tracked channel $\widehat{h}_v$. Fig. 5 shows the NMSE as a function of the SNR for $K = 2$, and $M = 70$. At 0dB and $\gamma = 1$, NMSE of the oracle OMP is -13.44dB, and NMSE of the proposed method is about -9.92dB. Also, channel tracking degrades the NMSE by about 3.5dB on average for $\gamma = 1$. We have observed that NMSE increases with time as the reconstruction error propagates for the successively tracked channels. In order to avoid accumulated error effect, channel estimation should be repeated in some well-defined intervals.

We expect NMSE to decrease as the number of measurement, M, increases. Fig. 6 shows that the NMSE increases approximately by about 1.74dB for $\gamma = 1$ when M is increased from 60 to 90.

SE **-** SE is defined by $SE = log_2\left[det\left(I + \frac{\rho}{\sigma}HH^H\right)\right]$ is the crucial performance metric for wireless systems. It determines how efficiently the proposed algorithm utilizes the bandwidth. In SE calculation, σ is the noise components contains the contribution of additive noise and the channel tracking error,

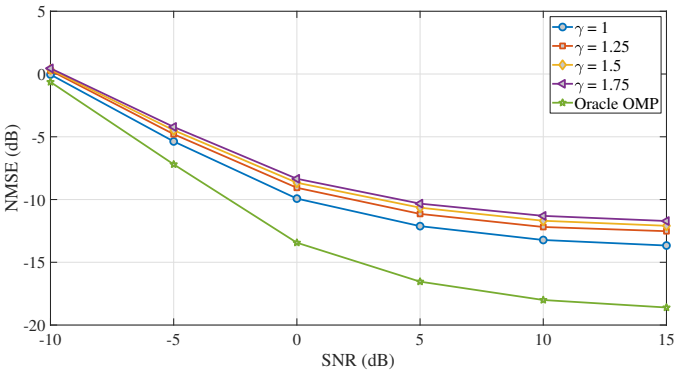

Fig. 5. NMSE as a function of SNR

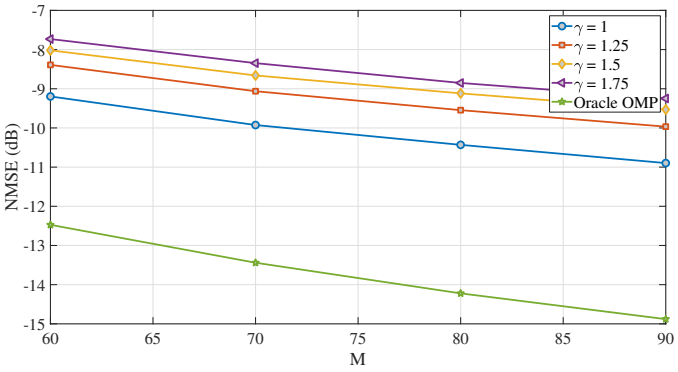

Fig. 6. NMSE as a function of number of measurements at 0dB SNR

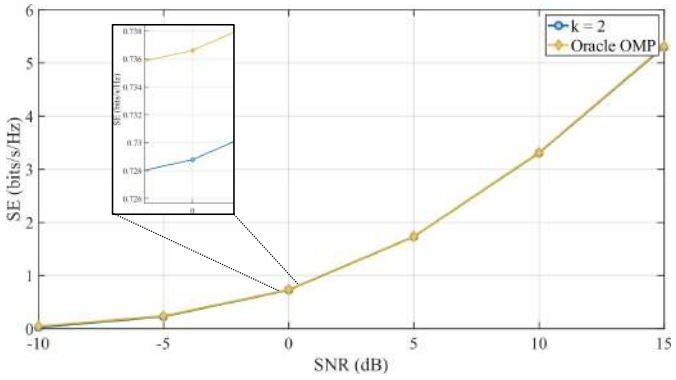

Fig. 7. Spectral efficiency as a function of SNR

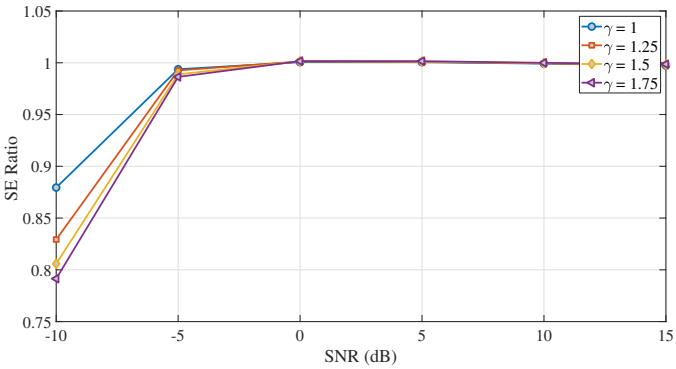

Fig. 8. Spectral efficiency preservation ratio as a function of SNR

ρ is the power, and H is the channel matrix. Fig. 7 shows the SE normalized by number of RF chains for $\gamma = 1.75$ and $M = 70$ as a function of the SNR. We can observe that the tracking stage has a minimal effect on the SE.

Fig. 8 shows SE ratio defined as $SE_{Raio} = \frac{SE_{Tr}}{SE_{Oracl\ Est}}$ as a function of SNR. According to the results, 87% of the SE achieved by oracle OMP is preserved by the proposed method.

Comparison with prior works - The OMP algorithm is widely used in the literature for millimeter-wave channel estimation. As shown in Fig. 5, the performance gap between the proposed method and oracle OMP algorithm increases as the SNR increases. This is mainly because the channel model in (10) only updates the AoD and AoA and disregards channel gain. However, at low SNR regimes, this gap decreases as the CMSV increases. This is due to the fact the number of estimated channels increases at the low SNR regimes and the proposed method approaches the oracle OMP.

We also have compared our results to [7, Fig. 2] for the four channel slots at 0dB. In [7], the recommended channel tracking method achieves approximately 0dB NMSE compared to -8.34dB we have measured. Here, the performance difference can be described by the different approaches used to update the AoD and AoA parameters.

V. Conclusion

In this paper, we proposed the adaptive channel estimation-tracking algorithm for continuous linear time-variant millimeter-wave massive MIMO. The dynamic behavior of the millimeter-wave channel is characterized using variation rate of the spectral overlap between successive channel realizations. We also proposed convergence in mean square to detect significant non-stationary events such as blockage. The results indicated that the proposed estimation-tracking algorithm achieves superior performance by minimizing the pilot overhead. The proposed method achieves NMSE as low as -13.44 at 0dB for 70 measurements. We also observed that at SNR as low as -10dB, 87% of the SE achieved by the oracle OMP has been preserved by the proposed method.

The proposed method has been evaluated under the spatial consistency where the mobility of the UT is limited to 3.6kps. Future works may examine and potentially optimize the proposed method for the scenarios with higher UT mobility and dual mobility. Potential applications include but not limited to multihop communication, and device-to-device communications.

VI. Appendix

Let's rephrase evolved channel transfer matrix in (9) as

$$H(t+\Delta t, f) = \sqrt{P_t N_r} \sum_{p=0}^{N-1} \sum_{l=0}^{L-1} \beta_{p,l}(t+\Delta t) \times \overline{a}_r(\theta_{p,l} + \Delta\theta_{p,l}) \overline{a}_t^H(\phi_{p,l} + \Delta\phi_{p,l}) \quad (15)$$

where $\beta_{p,l}(t+\Delta t) = \alpha_{p,l}(t+\Delta t)e^{j2\pi\upsilon_{p,l}t}e^{-j2\pi f\tau_{p,l}}$. Preposition 1 can be proved in two steps. In the first step, we need to prove that for all $p \in \{1,2,\cdots,N\}$ and $l \in \{1,2,\cdots,L\}$

$$\overline{a}_t(\theta+\Delta\theta) = \overline{a}_t(\theta) \circ \overline{a}_{\Delta\theta} \tag{16}$$

$$\overline{a}_r(\varphi+\Delta\varphi) = \overline{a}_r(\varphi) \circ \overline{a}_{\Delta\varphi} \tag{17}$$

In the second step, we nee to prove

$$\left(\overline{a}_r(\varphi) \circ \overline{a}_{\Delta\varphi}\right)\left(\overline{a}_t(\theta) \circ \overline{a}_{\Delta\theta}\right)^H = \left(\overline{a}_r(\varphi)\overline{a}_t(\theta)^H\right) \circ \left(\overline{a}_{\Delta\varphi}\overline{a}_{\Delta\theta}^H\right) \tag{18}$$

Proof: *Step 1:* From (2),for a given angle ϕ (ϕ can be $theta$ or ϕ), we will have

$$\overline{a}\left(\phi+\Delta\phi\right) = \left[1, e^{-j2\pi\frac{d}{\lambda}\sin(\phi+\Delta\phi)}, \cdots, e^{-j2\pi\frac{(N_t-1)d}{\lambda}\sin(\phi+\Delta\phi)}\right] \tag{19}$$

For small $\Delta\phi$, $cos(\Delta\phi) = 1$ and $\lim\frac{\sin(\Delta\phi)}{\Delta\phi} = 1$. Hence, we have

$$\sin(\phi+\Delta\phi) = \sin(\phi) + \Delta\phi\cos(\phi) \tag{20}$$

Substituting (20) in (19)

$$\begin{aligned}\overline{a}\left(\phi+\Delta\phi\right) = &\left[1, e^{-j2\pi\frac{d}{\lambda}\sin(\phi)}, \cdots, e^{-j2\pi\frac{(N_t-1)d}{\lambda}\sin(\phi)}\right] \circ \\ &\left[1, e^{-j2\pi\frac{d}{\lambda}\Delta\phi\cos(\phi)}, \cdots, e^{-j2\pi\frac{(N_t-1)d}{\lambda}\Delta\phi\cos(\phi)}\right] \\ &= \overline{a}(\phi) \circ \overline{a}_{\Delta\phi}\end{aligned} \tag{21}$$

Step 2: To prove (18), we use the following properties of the Hadamard product in a given order:(1) $(A \circ B)C = AC \circ B$, (2) $(A \circ B)^H = A^H \circ B^H$, (3) $A(B \circ C) = AB \circ C$, and (4) $A \circ B = B \circ A$.

$$\begin{aligned}\left(\overline{a}_r(\varphi) \circ \overline{a}_{\Delta\varphi}\right)\left(\overline{a}_t(\theta) \circ \overline{a}_{\Delta\theta}\right)^H &= \overline{a}_r(\varphi)\left(\overline{a}_t(\theta) \circ \overline{a}_{\Delta\theta}\right)^H \circ \overline{a}_{\Delta\varphi} \\ &= \overline{a}_r(\varphi)\left(\overline{a}_t(\theta)^H \circ \overline{a}_{\Delta\theta}^H\right) \circ \overline{a}_{\Delta\varphi} \\ &= \left(\overline{a}_r(\varphi)\overline{a}_t(\theta)^H\right) \circ \overline{a}_{\Delta\theta}^H \circ \overline{a}_{\Delta\varphi} \\ &= \left(\overline{a}_r(\varphi)\overline{a}_t(\theta)^H\right) \circ \overline{a}_{\Delta\varphi} \circ \overline{a}_{\Delta\theta}^H\end{aligned} \tag{22}$$

Substituting (22) into (15), we can prove (11) for $\omega \in \Omega$ as in the forward:

$$\begin{aligned}H(t+\Delta t, f) = \sqrt{N_t N_r}\sum_{p=0}^{N-1}\sum_{l=0}^{L-1}&\beta_{p,l}(t+\Delta t) \\ &\times\overline{a}_r(\varphi_{p,l})\overline{a}_t^H(\theta_{p,l}) \\ &\circ\overline{a}_{\Delta\varphi_\omega} \circ \overline{a}_{\Delta\theta_\omega}^H \\ &= H(t,f) \circ \overline{a}_{\Delta\varphi_\omega} \circ \overline{a}_{\Delta\theta_\omega}^H\end{aligned} \tag{23}$$

ACKNOWLEDGMENT

Computational resources were provided by the University of North Texas High-Performance Computing Services, a division of the Research IT Services, University Information Technology, with additional support from UNT Office of Research and Economic Development.

REFERENCES

[1] ETSI, "TS 138 104 - V15.2.0 - 5G; NR; Base Station (BS) radio transmission and reception (3GPP TS 38.104 version 15.2.0 Release 15)," *Online Available*, vol. 0, 2018. [Online]. Available: https://portal.etsi.org/TB/ETSIDeliverableStatus.aspx

[2] E. Björnson, J. Hoydis, and L. Sanguinetti, "Massive MIMO networks: Spectral, energy, and hardware efficiency," *Foundations and Trends® in Signal Processing*, vol. 11, no. 3-4, pp. 154–655, 2017. [Online]. Available: http://dx.doi.org/10.1561/2000000093

[3] Z. Gao, C. Hu, L. Dai, and Z. Wang, "Channel Estimation for Millimeter-Wave Massive MIMO with Hybrid Precoding over Frequency-Selective Fading Channels," *IEEE Communications Letters*, vol. 20, no. 6, pp. 1259–1262, 2016.

[4] M. Robaei and R. Akl, "Time-variant broadband mmwave channel estimation based on compressed sensing," in *2019 IEEE 10th Annual Ubiquitous Computing, Electronics & Mobile Communication Conference (UEMCON)*. IEEE, 2019, pp. 0172–0178.

[5] K. Venugopal, A. Alkhateeb, N. Gonzalez Prelcic, and R. W. Heath, "Channel Estimation for Hybrid Architecture-Based Wideband Millimeter Wave Systems," *IEEE Journal on Selected Areas in Communications*, vol. 35, no. 9, pp. 1996–2009, 2017.

[6] C. Zhang, D. Guo, and P. Fan, "Tracking angles of departure and arrival in a mobile millimeter wave channel," *2016 IEEE International Conference on Communications, ICC 2016*, pp. 1–6, 2016.

[7] J. Rodriguez-Fernandez, N. Gonzaiez-Prelcic, and R. W. Heath, "Frequency-domain wideband channel estimation and tracking for hybrid MIMO systems," *Conference Record of 51st Asilomar Conference on Signals, Systems and Computers, ACSSC 2017*, vol. 2017-Octob, pp. 1829–1833, 2018.

[8] Y. Wang, Z. Shi, L. Huang, Z. Yu, and C. Cao, "An extension of spatial channel model with spatial consistency," *IEEE Vehicular Technology Conference*, pp. 1–5, 2017.

[9] S. Ju, O. Kanhere, Y. Xing, and T. S. Rappaport, "A Millimeter-Wave Channel Simulator NYUSIM with Spatial Consistency and Human Blockage," pp. 1–6, 2019. [Online]. Available: http://arxiv.org/abs/1908.09762

[10] E. Zochmann, V. Va, M. Rupp, and R. W. Heath, "Geometric Tracking of Vehicular mmWave Channels to Enable Machine Learning of Onboard Sensors," *2018 IEEE Globecom Workshops, GC Wkshps 2018 - Proceedings*, 2019.

[11] E. Bonek, M. Herdin, and E. Bonek, "Correlation matrix distance , a meaningful measure for evaluation of non-stationary MIMO channels Correlation Matrix Distance , a Meaningful Measure for Evaluation of Non-Stationary MIMO Channels," *2005 IEEE 61st Vehicular Technology Conference*, vol. 1, no. February, pp. 136–140 Vol. 1, 2016.

[12] M. Robaei and R. Akl, "Examining spatial consistency for millimeter-wave massive MIMO channel estimation in 5G-NR," *Digest of Technical Papers - IEEE International Conference on Consumer Electronics*, vol. 2020-Janua, pp. 1–6, 2020.

[13] A. M. Sayeed, "Deconstructing multiantenna fading channels," *IEEE Transactions on Signal Processing*, vol. 50, no. 10, pp. 2563–2579, 2002.

[14] Y. Pati, R. Rezaiifar, and P. Krishnaprasad, "Orthogonal matching pursuit: recursive function approximation with applications to wavelet decomposition," pp. 40–44, 2002.

[15] M. Robaei and R. Akl, "Integrated map-statistical blockage modeling and mitigation for millimeter-wave communication," *ACM/IEEE Information Processing in Sensor Network*, 2021, manuscript submitted for publication.